Available online at www.sciencedirect.com
ScienceDirect
Journal of Power Sources 172 (2007) 597–603
JOURNAL OF POWER SOURCES
www.elsevier.com/locate/jpowsour

Evaluation of carbon-supported ruthenium-selenium-tungsten catalysts for direct methanol fuel cells

H. Cheng [a,*], W. Yuan [a], K. Scott [a], D.J. Browning [b], J.B. Lakeman [b]

[a] School of Chemical Engineering & Advanced Materials, Newcastle University, Newcastle upon Tyne NE1 7RU, UK
[b] Physical Sciences Department, Defence Science and Technology Laboratory, Porton Down, Salisbury, Wiltshire SP4 0QR, UK

Received 6 February 2007; received in revised form 16 April 2007; accepted 15 May 2007
Available online 21 May 2007

Abstract

The use of ruthenium-selenium-tungsten catalysts as methanol tolerant cathodes for direct methanol fuel cells is reported. The novel catalysts were produced by decarbonylation of ruthenium and tungsten carbonyls in the presence of selenium and carbon powders. The produced materials were characterised in both half cells and fuel cells. The addition of tungsten led to better oxygen reduction performance, giving current densities up to 30% greater and cell power densities up to 25% greater than those obtained with ruthenium-selenium alone. There is only a minor loss in methanol tolerance in the presence of tungsten. The improvement in performance is a consequence of the beneficial influence of tungsten on the structure and properties of catalysts. The effects of fuel cell operating conditions are also reported. The new catalysts were compared to Pt.

Keywords: Direct methanol fuel cells; Oxygen reduction; Methanol tolerant cathodes; Ruthenium-selenium-tungsten catalyst

1. Introduction

The direct methanol fuel cell (DMFC) has been identified as one of the alternatives to fossil fuel based combustion engines due to its increased fuel efficiency and low operating temperatures, without releasing toxic substances such as NO_x and SO_x. It is also seriously considered as a competitive stationary and portable power source [1–4]. However, there are several obstacles which restrict the cell performance, e.g. the slow oxygen reduction and poisoning of the platinum cathode by methanol crossover. This stimulates greater efforts to find alternatives to platinum. In this regard, ruthenium-based catalysts, formed from a combination of transition metals (e.g. Ru, Mo, Rh and Re) and chalcogens (e.g. Se and S), have shown reasonably high activity and high methanol tolerance [5–16]. The quaternary ruthenium-selenium-tungsten-tin catalysts also showed higher activity than the ruthenium-selenium-molybdenum catalysts, although there are few details available about the quaternary catalysts. Their methanol tolerance has not been mentioned and they have not yet been tested in the DMFC [17].

In general, the overall performance of ruthenium-based catalysts is still inferior to that of platinum under typical fuel cell conditions, which hinders their commercial application and implies requirements for a further improvement. To follow this direction, the present work modified ruthenium-selenium catalysts through the addition of another potential active component, i.e. tungsten.

Tungsten has shown activity for oxygen reduction [18]. Tungsten oxides are active for the reduction of hydrogen peroxide and were used as cathode supports [19,20]. For example, the carbon-supported RuSe cathode catalyst was modified by WO_3 for polymer electrolyte membrane fuel cells (PEMFC). The product was evaluated using the rotating disk electrode technique, which exhibited an increased activity towards the reduction of hydrogen peroxide [19]. However, the main application of tungsten oxides is as co-catalysts and/or supports for anode in both PEMFCs [21–25] and DMFCs [26–30]. Tungsten carbide is of interest as a cathode catalyst [31–34]; a carbon-supported tungsten carbide-silver material was reported to be active for oxygen reduction in alkaline media and was tolerant to alcohols [33].

Overall, most tungsten-containing cathode catalysts have only been tested in half cells [18–20]. A detailed assessment of them under fuel cell conditions is important because the catalyst performance greatly relies upon methods of manufac-

* Corresponding author. Tel.: +44 1912225206; fax: +44 1912225292.
E-mail address: hua.cheng@ncl.ac.uk (H. Cheng).

0378-7753/$ – see front matter © 2007 Elsevier B.V. All rights reserved.
doi:10.1016/j.jpowsour.2007.05.038

turing the electrode and membrane electrode assembly and upon the operation conditions. There is also a concern about the maintenance and recovery of tungsten oxides under a hostile cathodic environment because they suffered from dissolution in acid media [28,29,35] and the reduction of tungsten oxide occurred even during a short-time voltammetric measurement [34]. These problems may affect the function and stability of oxide-containing catalysts, particularly for a long-term application. Moreover, there are some unknown aspects for this type of catalyst, such as the effect of tungsten and tungsten compounds on methanol tolerance, even under half cell conditions. This was not a subject for PEMFCs [19], but as cathode components for DMFCs, this seems a concern because, for example, the presence of tungsten oxides led to the increased rate of methanol oxidation [26]. Therefore, as a part of the work in this lab to alleviate negative effects of methanol crossover on the cell performance, a new approach different to that published in Ref. [19] has been taken to modify ruthenium-selenium catalysts; i.e. by decarbonylation of tungsten carbonyls in xylene rather than using tungsten trioxide. Furthermore, the produced ruthenium-selenium-tungsten catalysts were thoroughly reduced under hydrogen atmosphere and examined for their electrochemical performance and were compared to ruthenium-selenium alone and to platinum in half-cells as well as in the DMFC. The data obtained are discussed in relation to the beneficial effect of tungsten on oxygen reduction.

2. Experimental

2.1. Catalyst preparation

The synthesis procedure was described elsewhere [5]; an example is given below. Selenium (0.04 g, 99%, Riedel-deHaen) was dissolved in 500 ml of boiling xylene (anhydrous, 97%, Aldrich) for 2 h. Carbonyls (0.5 g $Ru_3(CO)_{12}$, 99%, Aldrich and 0.24 g $W(CO)_6$, 97%, Aldrich) were then added to the solution and refluxed for 12 h. Finally, carbon powder (0.3 g, Vulcan XC-72R, Cabot) was added to the solution and refluxed for another 20 h. The solution was bubbled with nitrogen gas (BOC) under mechanical stirring throughout the procedure. The products were filtered, washed with dry ether and dried overnight; then annealed at 360 °C for 1 h under 0.1 l min^{-1} hydrogen (BOC) before being cooled to room temperature at 0.1 l min^{-1} nitrogen. The product formula is $RuSe_{0.20}W_{0.29}$ determined by the EDX measurement.

2.2. Half cell test

The half cell test was carried out in a one-compartment three-electrode cell (200 cm^3 in volume) with a double wall for the circulation of water from a temperature controlled bath. The circular working gas diffusion electrode (1 cm^2) and a Pt mesh (20 cm^2, 99.99%, Goodfellow) counter electrode were placed within the cell. An Hg/Hg_2SO_4 (saturated K_2SO_4) reference electrode (Russell) was connected to the cell through a Luggin capillary with a glass frit separator. The working electrodes had a loading of 1 mg RuSe cm^{-2}. A Pt electrode (1 mg Pt cm^{-2}, using 60 wt.% Pt on Vulcan XC-72R, E-TEK) was also used for comparison. They were prepared by pasting a mixture of the catalyst and Nafion (30 mass% of the overall catalyst weight using 5 mass% Nafion solution from Aldrich) in iso-propanol onto the carbon paper (TGPH120, E-TEK). After hot-pressing at 100 kg cm^{-2} and 130 °C, the electrodes were mounted in a PTFE holder, which allowed gasses to pass at the rear-side of the electrode and to penetrate into solution via the front face of the electrode.

Cyclic voltammetry and potential-step chronoamperometric polarisation were performed using a VoltaLab 50 potentiostat (PST050 & VoltaMaster 4, Radiometer). The electrolyte was a 0.5 M H_2SO_4 (AnalaR, BDH) solution, with and without methanol (99.99%, Fisher), prepared using deionised water (ELGASTAT B124 Water Purification Unit, the Elga Group, England). All working electrodes were pre-treated by cycling in 0.5 M H_2SO_4 solution between 0.3 and −1.0 V for 50 cycles at a scan rate of 50 mV s^{-1}. Thereafter, the gas diffusion electrode was fed either with oxygen (BOC) or with nitrogen at a flow rate of 25 cm^3 min^{-1} under atmospheric pressure.

2.3. Fuel cell test

The gas diffusion layers were made using Ketjen-300J carbon black (1 mg cm^{-2}, Akzo Nobel), Teflon (20 mass% Teflon of the overall catalyst weight, Aldrich) and a carbon paper (Toray, TGPH120, E-TEK). Nafion® ionomer (15 mass% of the overall catalyst weight) and iso-propanol were used to prepare inks for catalytic layers. Catalyst loadings were 1.52 mg PtRu cm^{-2} for anodes (using 60 wt.% PtRu on Vulcan XC-72R with the atomic ratio of Pt to Ru 1:1, E-TEK) and 2 mg RuSe or Pt cm^{-2} for cathodes. The desired amounts of catalyst materials were weighed for each electrode before making membrane electrode assemblies. Finally, a thin layer of Nafion (1 mg cm^{-2}) solution was spread onto the electrode surface. Membrane electrode assemblies were obtained by pressing the anode and cathode on either side of a Nafion® 117 membrane (DuPont) under a pressure of 50 kg cm^{-2} at 130 °C for 3 min.

The DMFC was assembled to allow good contact between electrodes and graphite blocks (Ralph, Coidan), into which the gas/liquid flow channels were cut. The total machined geometrical area of 4 cm^2 was taken as the active area of the cell. Copper sheets contacted the graphite blocks as current collectors. Electrical heaters were mounted at the rear of the Cu plates to maintain desired cell temperature. The temperature was controlled through a temperature controller and monitored by thermocouples buried in the graphite blocks. Steady-state polarisation measurements were carried out following 2 days conditioning, during which the cell was held at 60 °C and fed with deionised water in order to hydrate the membrane. Polarisation curves were recorded in a galvanostatic mode, starting from open circuit point and moving to higher current densities. A stable period was allowed at each current density before recording data, which was approximately 3 min in most cases.

Other experimental details, including the details of X-ray diffraction (XRD) measurements, have been described in Ref. [5]. The XRD patterns were compared to the International Centre for Diffraction Data® (ICDD®) [36].

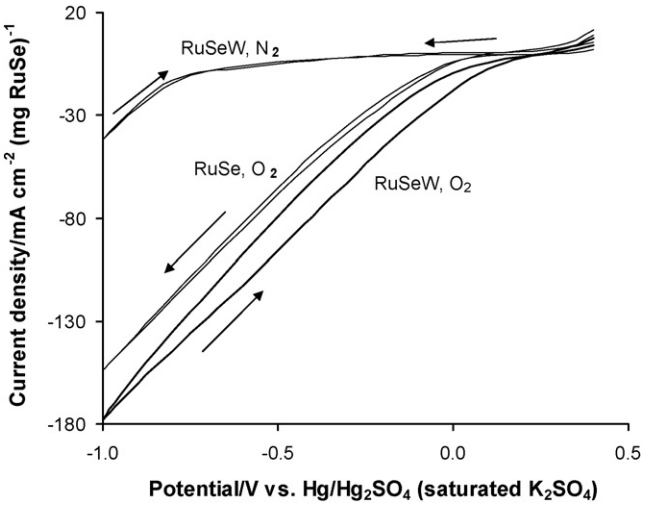

Fig. 1. Cyclic voltammograms on the carbon-supported $RuSe_{0.19}$ and $RuSe_{0.20}W_{0.29}$ (1 mg RuSe or Pt cm^{-2}) gas diffusion electrodes. Undivided glass cell. Electrode area: 1 cm^2. Electrolyte: 0.5 M H_2SO_4 solution saturated with N_2 or O_2. Scan rate: 5 mV s^{-1}. Temperature: 25 °C. The scan directions were indicated by the arrows.

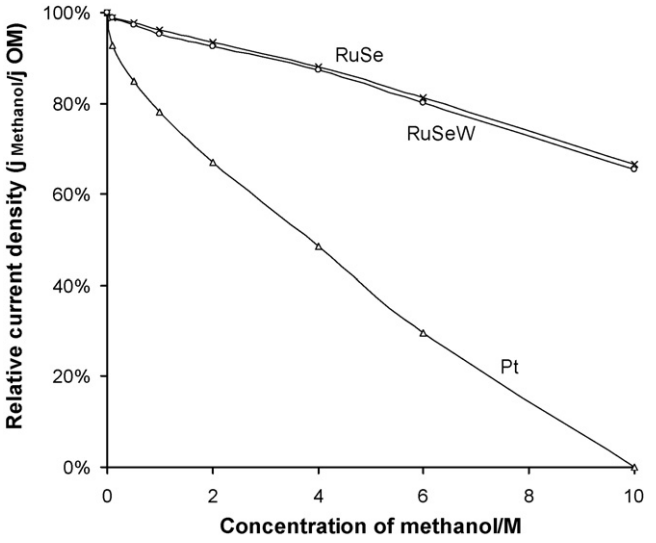

Fig. 2. Relative current density against methanol concentration curves for the $RuSe_{0.19}$, $RuSe_{0.20}W_{0.29}$ and Pt gas diffusion electrodes. Electrolyte: a solution of 0.5 M H_2SO_4 with and without methanol purged with oxygen. Methanol concentration: 0.1, 0.5, 1, 2, 4, 6 and 10 M. Other conditions as in Fig. 1.

3. Results and discussion

3.1. Half cell test

3.1.1. Catalytic activity

Fig. 1 compares the cyclic voltammograms for the carbon-supported $RuSe_{0.19}$ and $RuSe_{0.20}W_{0.29}$ gas diffusion electrodes. The $RuSe_{0.20}W_{0.29}$ cathode is active for oxygen reduction, as indicated by higher current densities at each potential in the O_2-saturated solution than those using N_2. More importantly, the activity of the $RuSe_{0.20}W_{0.29}$ is greater than that of $RuSe_{0.19}$, suggesting by higher current densities at a given potential, e.g. 79 against 65 mA cm^{-2} at −0.5 V. This clearly shows the beneficial effect of tungsten modification on the activity of the Ru-based catalysts. The negative currents are still observed during the reverse scans, which is an indication of the high irreversibility of oxygen reduction.

As can be seen, there is a large voltage window for oxygen reduction for both electrodes. This can be attributed to several aspects, such as the segregated ribbon-like channel structure and high catalyst dispersion on gas diffusion electrodes, leading to high catalyst utilisation. The use of hydrophobic agents (e.g. PTFE) also rejects water and creates an extended aqueous thin layer between the electrolyte and gas phase, which greatly reduces the mass transport barrier. As a consequence, a three-phase (electrode/electrolyte/gas) boundary region is produced. This extends reaction zones, leading to significantly larger surface areas, compared to other solid electrodes (e.g. disks, rods and flat sheets, etc.) where only the electrode/electrolyte two-phase boundaries are available [37,38].

3.1.2. Methanol tolerance

The effect of tungsten modification on methanol tolerance of Ru-based catalysts was assessed thoroughly in solutions with varying methanol concentrations using the potential-step chronoamperometric technique. The loss of activity due to the methanol poisoning is compared based on a relative current density drop for each electrode, which is a ratio of any current density in the presence of methanol to that without methanol at a potential of −0.4 V versus Hg/Hg_2SO_4 (saturated K_2SO_4), i.e. $j_{Methanol}/j_{0M}$. Here j_{0M} and $j_{Methanol}$ (mA cm^{-2}) are absolute values of the net current density in the blank and methanol solutions.

Fig. 2 shows typical data collected at −0.4 V versus Hg/Hg_2SO_4 (saturated K_2SO_4), including the data for the Pt electrode for comparison. The relative current density decreases

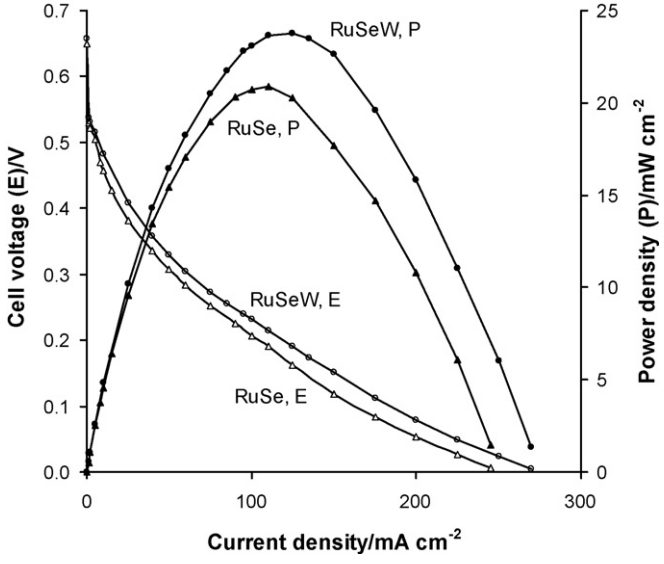

Fig. 3. Effect of tungsten addition on the performance of the DMFCs with the carbon-supported $RuSe_{0.19}$ and $RuSe_{0.20}W_{0.29}$ cathodes (2 mg RuSe cm^{-2}). Active area: 4 cm^2. Anode: carbon-supported PtRu (1.52 mg PtRu cm^{-2}). Membrane: Nafion® 117. Fuel: 1 M methanol (10 cm^3 min^{-1}). Oxidant: O_2 (200 cm^3 min^{-1}, ambient pressure). Temperature: 90 °C.

with increasing methanol concentration for both Ru-based catalysts, suggesting that they are not completely tolerant to methanol. The $RuSe_{0.20}W_{0.29}$ shows higher reduction current density than $RuSe_{0.19}$, even in the 4 M methanol solution (i.e. 56 mA cm^{-2} versus 52 mA cm^{-2} from the chronoamperometric measurement); however, its methanol tolerance is slightly reduced, as indicated by its lower relative current densities at each methanol concentration, compared to $RuSe_{0.19}$ (Fig. 2). In contrast, the Pt catalyst shows a greater deterioration in relative current density than other catalysts, suggesting its lower methanol tolerance.

3.2. Fuel cell evaluation

3.2.1. Influence of tungsten modification

A performance comparison is made for the DMFCs with the $RuSe_{0.19}$ and $RuSe_{0.20}W_{0.29}$ cathodes, as shown in Fig. 3. The MEA with the $RuSe_{0.20}W_{0.29}$ cathode gives better performance than that with $RuSe_{0.19}$, e.g. approximately 25 mV higher in cell voltage at a current density of 100 mA cm^{-2}. The results demonstrate that the activity of Ru-based catalysts can be improved by the tungsten modification.

3.2.2. Influence of fuel conditions

It is interesting to compare the relationship between cell performance and methanol concentration for the DMFCs with the $RuSe_{0.20}W_{0.29}$ and Pt cathodes. As shown in Fig. 4a, the DMFC with the Pt cathode shows superior performance to that with the $RuSe_{0.20}W_{0.29}$ using 2 M fuel, e.g. 0.32 V versus 0.24 V in cell voltage and 32 against 24 mW cm^{-2} in power density at 100 mA cm^{-2}. The order is reversed when 4 M methanol is used; the Pt is inferior to the $RuSe_{0.21}W_{0.28}$ cathode, e.g. 0.19 V versus 0.25 V and 19 against 25 mW cm^{-2} also at 100 mA cm^{-2} (Fig. 4b). Using 10 M methanol, the peak power density of

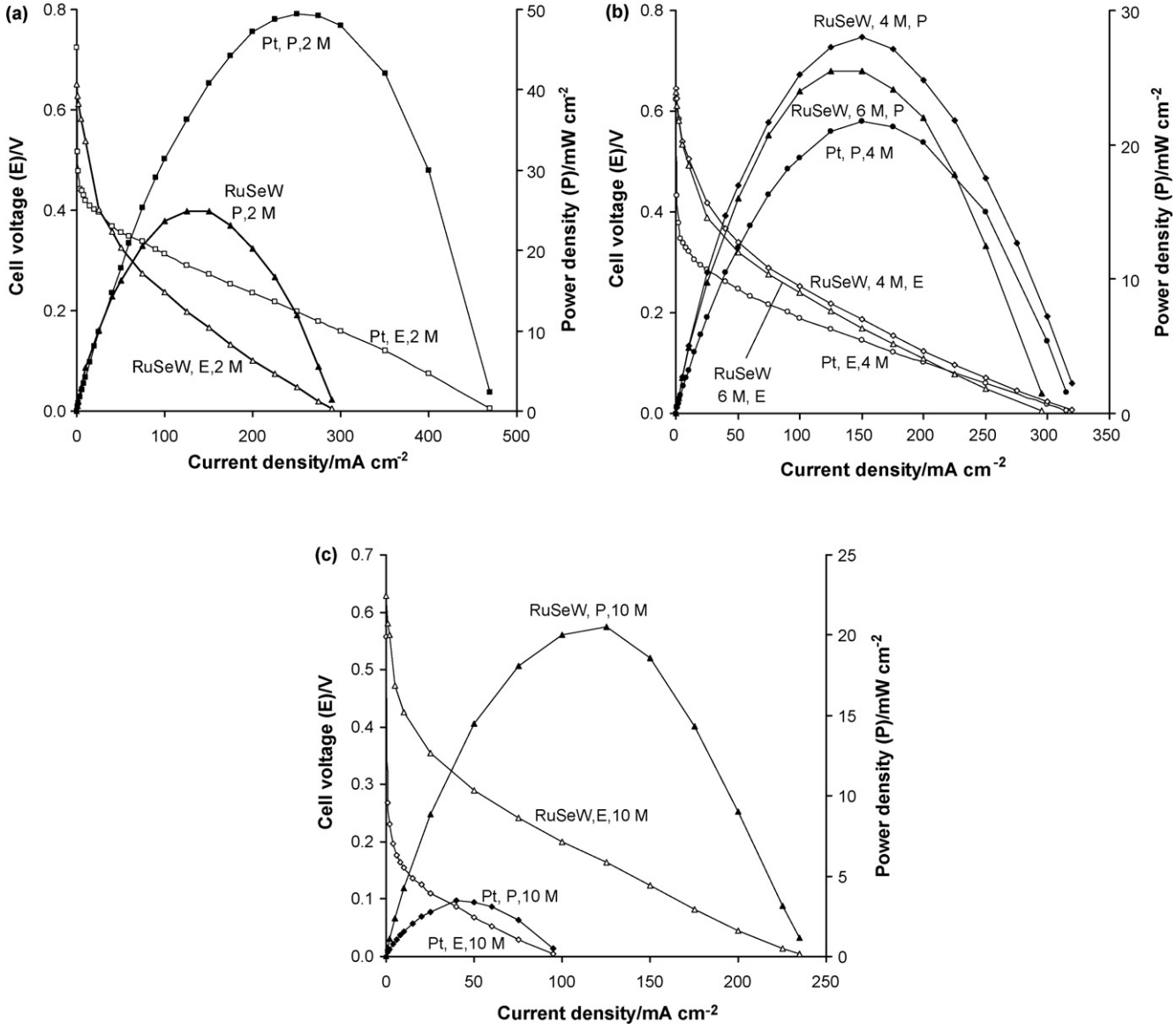

Fig. 4. The performance comparison for the DMFCs with the $RuSe_{0.20}W_{0.29}$ and Pt (2 mg Pt cm^{-2}) cathodes. Fuel: 2 M (a), 4 and 6 M (b) and 10 M (c) methanol (10 cm^3 min^{-1}). Other conditions as in Fig. 3.

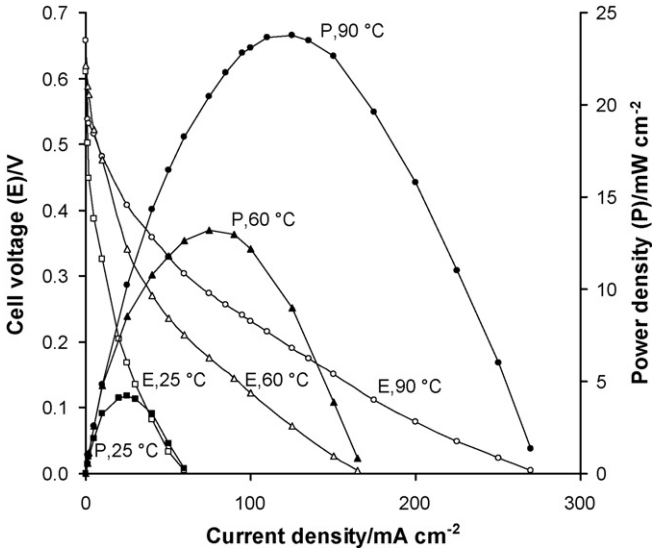

Fig. 5. Effect of temperature on the performance of the DMFC with the carbon-supported $RuSe_{0.20}W_{0.29}$ cathode. Fuel: 1 M methanol (10 cm^3 min^{-1}). Other conditions as in Fig. 3.

the DMFC with the Pt cathode is only 20% of that with $RuSe_{0.20}W_{0.29}$ (Fig. 4c). The data illustrate the significantly higher methanol tolerance of the $RuSe_{0.20}W_{0.29}$ catalyst than Pt.

On the other hand, Pt is still superior to the Ru-based catalysts in terms of their best performances. As shown in Fig. 4, using ambient oxygen, the maximum peak power density for the DMFCs with the Pt cathode is 50 mW cm^{-2} (Fig. 4a) but only 28 mW cm^{-2} for that with the $RuSe_{0.20}W_{0.29}$ cathode (Fig. 4b). This indicates that the new catalysts need to be improved, especially for low concentration applications.

As expected, the higher the cell temperature, the better the performance (Fig. 5), due to the enhanced electrode kinetics. The enhanced negative effects of the increased vapour pressure of water and methanol crossover with increasing temperature seem to be counteracted by the thermal activation.

3.2.3. Influence of oxidants

Fig. 6a shows the influence of the oxidant conditions on the cell performance collected using the DMFC with the $RuSe_{0.20}W_{0.29}$ cathode. Higher power densities are observed by using oxygen rather than air, e.g. 28 mW cm^{-2} versus 16 mW cm^{-2} for 4 M methanol, mainly due to the less mass transport problem when oxygen is used. A further increase in power density is achieved at high pressures, as shown in Fig. 6b, e.g. 39.5 mW cm^{-2} at 2 bar oxygen. This is due to an increase in oxidant supply concentration, which leads to the increased reversible cathode potential, decreased diffusion polarisation of cathode and enhanced kinetics of oxygen reduction. The improved performance is also a consequence of the increased oxidant access and reduction in ohmic losses because the porous structure might be prevented from flooding under pressurised conditions.

A comparison of the $RuSe_{0.20}W_{0.29}$ cathode with $RuSe_{0.19}$ (Fig. 6b) shows that the former has better performance under pressurised conditions in terms of, for example, peak power

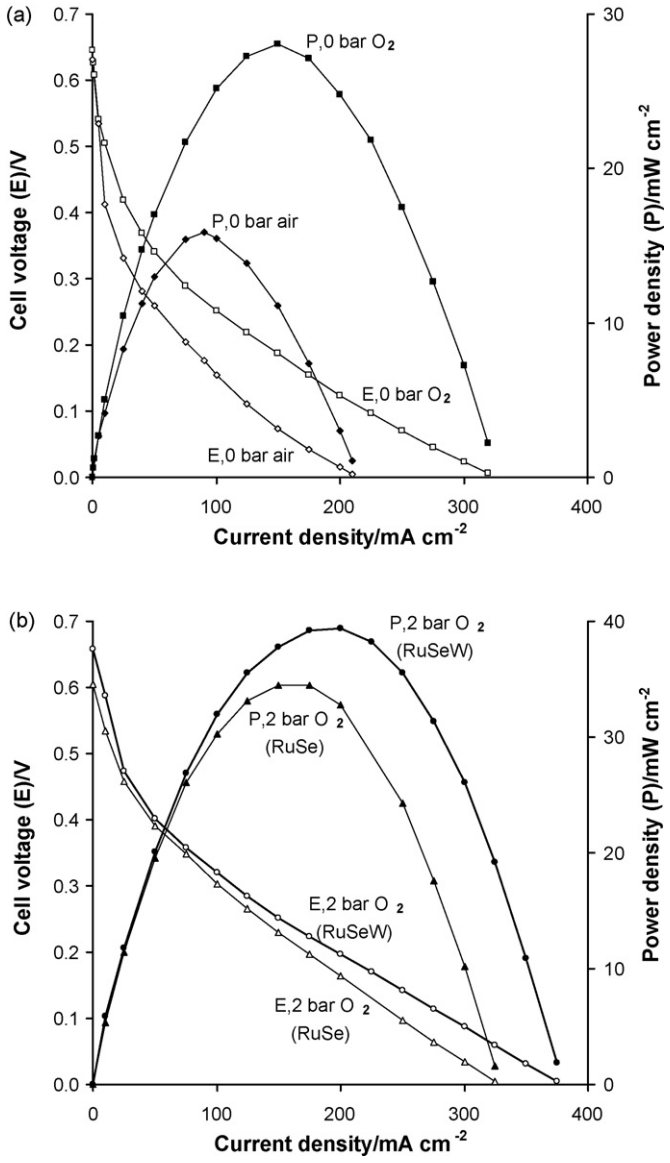

Fig. 6. Effect of oxidants on the DMFC performance. (a) 0 bar air and O_2, $RuSe_{0.20}W_{0.29}$ cathode; (b) 2 bar O_2, $RuSe_{0.19}$ and $RuSe_{0.20}W_{0.29}$ cathodes. Fuel: 4 M methanol (10 cm^3 min^{-1}). Other conditions as in Fig. 3.

density. This demonstrates again the beneficial effect of tungsten addition on the catalyst activity.

3.3. Discussion

The improved catalyst activity in the presence of tungsten is attributable to a combined effect, such as:

(a) Co-catalytic effect: Tungsten itself shows activity for oxygen reduction [18]. Moreover, our work [39] shows that the tungsten addition leads to higher exchange current densities and lower activation energies for oxygen reduction, compared to the absence of tungsten, suggesting a co-catalytic effect of tungsten.
(b) Chemical effects: The weight loss experiments showed a less loss in Se due to the presence of tungsten, e.g. 15%

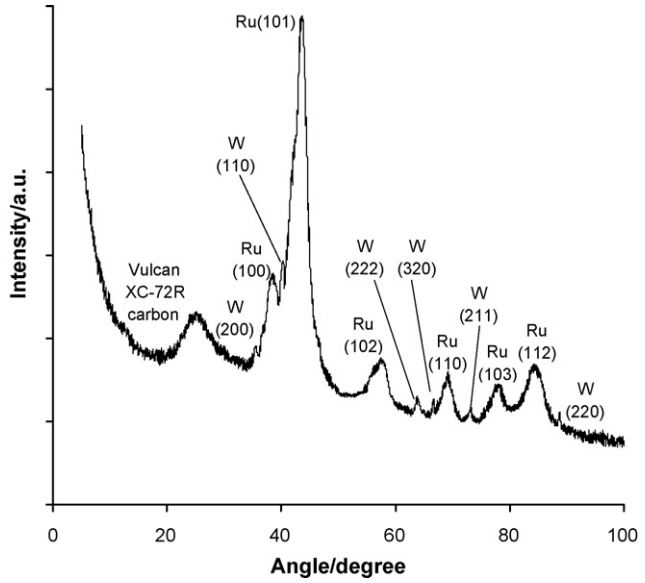

Fig. 7. X-ray diffraction (XRD) patterns of the carbon-supported $RuSe_{0.20}W_{0.29}$ material.

versus 5% for the $RuSe_{0.19}$ and $RuSe_{0.20}W_{0.29}$ samples, respectively. This means that the addition of tungsten has a stabilising effect on Se, which in turn facilitates the oxygen adsorption on the RuSeW catalyst and a better electron transfer between reactants and the catalyst active sites as a consequence of the beneficial influences of Se on electron transfer and oxygen adsorption [5,10,40].

(c) Structural effects: As shown in Fig. 7, the XRD patterns of the carbon-supported RuSeW material predominantly consist of the crystalline hexagonal ruthenium and cubic tungsten phases. The peaks may be assigned to the crystal faces of W(2 0 0), W(1 1 0), W(2 2 2), W(3 2 0), W(2 1 1) and W(2 2 0) at 2θ of 35.5°, 40.3°, 63.8°, 66.7°, 73.2° and 87.0°, respectively [36]; and to those of Ru(1 0 0), Ru(1 0 1), Ru(1 0 2), Ru(1 1 0), Ru(1 0 3) and Ru(1 1 2) peaks at 2θ of 38.4°, 44.0°, 58.3°, 69.4°, 78.4° and 84.7°, respectively [36]. No distinctive Se phases were observed in the XRD patterns, most likely due to the overlap between the peaks of Ru and Se [36]. It also cannot rule out the possibility that Se exists in the RuSeW catalyst as very fine nanocrytals with low intensity since the EDX measurements confirmed the presence of Se. The broad peak at ca. 25° is the reflection of Vulcan XC-72R carbon black support. Such crystal structures have a beneficial influence on the catalyst activity towards oxygen reduction because the crystal faces of tungsten, e.g. the W(1 1 0) crystal face, were believed to be favourable sites for the chemisorptions of oxygen [41,42].

The XRD measurements also proved the metal states of W and Ru, suggesting that the catalyst surface is not covered by oxides, which in turn facilitates adsorption and activation of oxygen molecules during electrocatalysis.

The SEM measurements showed that the RuSeW catalyst has smaller particle sizes (60–250 nm) than RuSe alone (60–350 nm) [39]. This indicates the decreased agglomeration of catalyst due to the presence of tungsten, leading to a higher surface area of catalyst, compared to the case without tungsten. Such a synergistic effect has the implication in the capability of providing more active sites for oxygen reduction.

In sum, the existence of the co-catalytic, chemical and structural effects lead to the formation of an efficient catalytic RuSeW system, which exhibits a higher electrochemical performance than RuSe alone.

It is worth using other techniques, such as X-ray photoelectron spectroscopy (XPS), in a further work in order to gain more insights into the surface structure, the electronic configuration and the catalytic mechanism of the RuSeW catalysts.

4. Conclusions

The activity of ruthenium-selenium catalysts towards oxygen reduction was increased by the tungsten modification. The tungsten addition led higher reduction currents than RuSe alone with only a minor effect on methanol tolerance. The DMFC with the RuSeW cathode delivered higher powers than that with RuSe. The RuSeW catalyst exhibited higher methanol tolerance than Pt, as suggested by the superior DMFC performance for methanol concentrations of 4 M or more.

Acknowledgements

The authors thank the EPSRC for funding and an EPSRC/HEFCE Joint Infrastructure Fund award (No. JIF4NESCEQ) for research facilities. We also thank P. Carrick (Chemical & Materials Analysis, Newcastle University) and K. Liddell (CEAM Advanced Materials Division, Newcastle University) for their technical assistance with the SEM, EDX and XRD measurements.

References

[1] N.P. Brandon, D. Thompsett, Fuel Cells Compendium, Elsevier, London, 2005.
[2] W. Vielstich, A. Lamm, H. Gasteiger (Eds.), Handbook of Fuel Cells: Fundamentals, Technology, Applications, vols. 3 and 4, John Wiley and Sons, New York, 2003.
[3] J. Laramie, A. Dicks, Fuel Cell Systems Explained, second ed., John Wiley and Sons, New York, 2003.
[4] R. Thring (Ed.), Fuel Cells for Automotive Applications, John Wiley and Sons, New York, 2003.
[5] H. Cheng, W. Yuan, K. Scott, Electrochim. Acta 52 (2006) 466.
[6] H. Schulenburg, M. Hilgendorff, I. Dorbandt, J. Radnik, P. Bogdanoff, S. Fiechter, M. Bron, H. Tributsch, J. Power Sources 155 (2006) 47.
[7] D. Cao, A. Wieckowski, J. Inukai, N. Alonso-Vante, J. Electrochem. Soc. 153 (2006) A869.
[8] N. Alonso-Vante, Handbook of fuel cells, in: W. Vielstich, H.A. Gasteiger, A. Lamm (Eds.), Electrocatalysis, vol. 2, John Wiley & Sons, New York, 2003, Chapter 36.
[9] M. Hilgendorff, K. Diesner, H. Schulenburg, P. Bogdanoff, M. Bron, S. Fiechter, J. New Mater. Electrochem. Syst. 5 (2002) 71.
[10] M. Bron, P. Bogdanoff, S. Fiechter, I. Dorbant, M. Hilgendorff, H. Schulenburg, H. Tributsch, J. Electroanal. Chem. 500 (2001) 510.
[11] R.W. Reeve, P.A. Christensen, A.J. Dickinson, A. Hamnett, K. Scott, Electrochim. Acta 45 (2000) 4237.
[12] T.J. Schmidt, U.A. Paulus, H.A. Gasteiger, N. Alonso-Vante, R.J. Behm, J. Electrochem. Soc. 147 (2000) 2620.

[13] R.W. Reeve, P.A. Christensen, A. Hamnett, S.A. Haydock, S.C. Roy, J. Electrochem. Soc. 145 (1998) 3463.
[14] V. Trapp, P.A. Christensen, A. Hamnett, J. Chem. Soc. Faraday Trans. 92 (1996) 4311.
[15] N. Alonso-Vante, H. Tributsch, O. Solorza-Feria, Electrochim. Acta 40 (1995) 567.
[16] N. Alonso-Vante, H. Tributsch, Nature (London) 323 (1986) 431.
[17] E. Reddington, J. Yu, A. Sapienza, B.C. Chan, B. Gurau, R. Viswanathan, R. Liu, E.S. Smotkin, S. Sarangapani, T.E. Mallouk, Adv. Catal. Mater. (Mat. Res. Soc. Symp. Proc.) 549 (1999) 231.
[18] M. Pattabi, R.H. Castellanos, R. Castillo, A.L. Ocampo, J. Moreira, P.J. Sebastian, J.C. McClure, X. Mathew, Int. Hydrogen Energy 26 (2001) 171.
[19] P.J. Kulesza, K. Miecznikowski, B. Baranowska, M. Skunik, S. Fiechter, P. Bogdanoff, I. Dorbandt, Electrochem. Commun. 8 (2006) 904.
[20] P.J. Kulesza, B. Grzybowska, M.A. Malik, M.T. Galkowski, J. Electrochem. Soc. 144 (1997) 1911.
[21] L. Gustavo, S. Pereira, F.R. dos Santos, M.E. Pereira, V.A. Paganin, E.A. Ticianelli, Electrochim. Acta 51 (2006) 4061.
[22] J. Shim, C.-R. Lee, H.-K. Lee, J.-S. Lee, E.J. Cairns, J. Power Sources 102 (2001) 172.
[23] M. Götz, H. Wendt, Electrochim. Acta 43 (1998) 3637.
[24] P.K. Shen, A.C.C. Tseung, J. Electrochem. Soc. 141 (1994) 3082.
[25] K. Machida, M. Enyo, G. Adachi, J. Shiokawa, J. Electrochem. Soc. 135 (1988) 1955.
[26] R. Ganesan, J.S. Lee, J. Power Sources 157 (2006) 217.
[27] E.J. McLeod, V.I. Birss, Electrochim. Acta 51 (2005) 684.
[28] V. Raghuveer, B. Viswanathan, J. Power Sources 144 (2005) 1.
[29] K.Y. Chen, A.C.C. Tseung, J. Electrochem. Soc. 143 (1996) 2703.
[30] P.K. Shen, P.K. Chen, A.C.C. Tseng, J. Chem. Soc. Faraday Trans. 90 (1994) 3089.
[31] X.G. Yang, C.Y. Wang, Appl. Phys. Lett. 86 (2005) 224104.
[32] R. Ganesan, J.S. Lee, Angew. Chem. Int. Ed. 44 (2005) 6557.
[33] H. Meng, P. Shen, Electrochem. Commun. 8 (2006) 588.
[34] K. Lee, A. Ishihara, S. Mitsushima, N. Kamiya, K. Ota, Electrochim. Acta 49 (2004) 3479.
[35] B. Reichman, A.J. Bard, J. Electrochem. Soc. 126 (1979) 583.
[36] The International Centre for Diffraction Data®, http://www.icdd.com/ (the reference codes are 06-0663 for Ru, 06-0362 for Se and 04-0806 and 047-1319 for tungsten).
[37] K. Kinoshita, Electrochemical Oxygen Technology, Wiley & Sons, New York, 1992, Chapter 3.
[38] L. Rabinovich, D. Lev, G.A. Tsirlina, J. Electroanal. Chem. 466 (1999) 45.
[39] H. Cheng, W. Yuan, K. Scott, D.J. Browning, J.B. Lakeman, Electrochemical reduction of oxygen on ruthenium-selenium-transition metal catalysts, accepted by the 58th International Society of Electrochemistry Annual Meeting, Banff, Canada, September 2007.
[40] H. Tributsch, M. Bron, M. Hilgendorff, H. Schulenburg, I. Dorbant, V. Eyert, P. Bogdanoff, S. Fiechter, J. Appl. Electrochem. 31 (2001) 739.
[41] H. Yamazaki, S. Kamimizu, K. Hara, K. Sakamoto, Surf. Sci. 538 (2003) L505.
[42] H. Yamazaki, T. Kamisawa, T. Kokubun, T. Haga, S. Kamimizu, K. Sakamoto, Surf. Sci. 477 (2000) 174.